Proceedings of GT2006
ASME Turbo Expo 2006: Power for Land, Sea and Air
May 8-11, 2006, Barcelona, Spain

GT2006-91338

STAGNATION-POINT REVERSE-FLOW COMBUSTOR PERFORMANCE WITH LIQUID FUEL INJECTION

John Crane, Yedidia Neumeier, Jeff Jagoda, Jerry Seitzman, and Ben T. Zinn
Georgia Institute of Technology, Department of Aerospace Engineering, Atlanta, Georgia 30332

ABSTRACT

This paper describes an investigation of the performance of the recently developed ultra low emissions, Stagnation-Point Reverse-Flow (**SPRF**) Combustor when burning liquid fuels (Jet-A and heptane). This study has been undertaken because of the need to burn liquid fuels with low emissions in gas turbines that are used, for example, in aircraft engines, land-based power generation, and marine applications. In contrast with state of the art combustors, in which the reactants and products enter and leave the combustor through opposite ends of the combustor, the reactants and products enter and leave the SPRF combustor through the same plane opposite a closed end. The design of the SPRF combustor allows mixing of reactants with hot combustion products and radicals within the combustor, prior to combustion. Thus, no external premixing of fuel and air is required. Additionally, since the air and fuel enter opposite the closed end of the combustor, they must stagnate near the closed end, thus establishing a region of low velocity just upstream of the closed end that helps stabilize the combustion process. This apparently produces a low temperature, stable, distributed reaction zone. Previous studies with the SPRF combustor investigated its performance while burning natural gas. This paper presents the results of SPRF combustor studies using liquid fuels, both heptane and Jet-A. The performance of the combustor was investigated using an airblast fuel injector, which is suitable for the low fuel flow rates used in laboratory experiments. To reduce pressure losses across the injector, a diffuser was incorporated into the airblast injector. It was found that stable combustor operation was achieved burning Jet-A with emissions of less than 1 ppm NO_x and 5 ppm CO, pressure losses less than 5 percent, and a power density on the order of 10 MW/m^3 in atmospheric pressure. This power density would linearly scale to 300 MW/m^3 in a combustor at a pressure of 30 atmospheres.

Keywords: stagnation point reverse flow combustor, SPRF combustor, liquid fuel, Jet-A, heptane, ultra-low, NOx, CO, emissions

INTRODUCTION

A significant fraction of combustion research during the past several decades has been devoted to minimizing pollutant emissions from combustion systems, notably nitrogen oxides (NO_x) and carbon monoxide (CO). Much of this research focused on limiting NO_x formation through the Zeldovich mechanism by keeping combustion temperatures low, typically below 1800 K. This research resulted in the development of several combustion approaches such as lean premixed combustion [1], external exhaust gas recirculation [2, 3], water injection [4], and internal combustion product recirculation [5], each with its own set of problems when used in gas turbines. More recently, a new approach, referred to as the Stagnation-Point Reverse-Flow (SPRF) combustor, for burning fuels with low emissions has been developed. It has been shown that the SPRF combustor can stably operate with ultra-low NO_x emissions when burning natural gas fuel [6] without encountering any of the problems that hindered the operation of combustors based upon the earlier developed approaches. While natural gas is a suitable fuel for many applications, e.g., land based power generation, there is also a need to develop effective means for burning liquid fuels, such as Jet-A, with ultra low emissions in a variety of applications including aircraft engines. This paper describes the performance of the SPRF combustor while burning such fuels.

When burning liquid fuels, a common problem in achieving low emissions is the attainment of proper atomization and distribution of the liquid fuel droplets within the combustor to produce a uniform, pseudo prevaporized-premixed fuel-air mixture. Additionally, for gas turbine applications, the pressure drop across the air injector must be small to improve overall cycle performance. Due to the low fuel flow rates associated with laboratory combustors, it is not possible to use pressure atomizers, which are traditionally used in liquid fuel combustion. For these studies, an airblast atomizer was used. Airblast atomization, though, is associated with high pressure losses. To maintain low pressure losses and optimal atomization, a venturi-type liquid fuel injector was developed and incorporated into the SPRF combustor.

EXPERIMENTAL SETUP

Figure 1 shows a schematic of the investigated SPRF combustor and flow pattern. It consists of a short tube with opposing closed and open ends and an injection system at the center of the open end, consisting of two coaxial tubes. The injection system, detailed in Fig. 2, right, supplies air through the annular space between the two tubes and liquid fuel through the central tube. The non-premixed reactants are injected along the combustor's center line towards its closed end, where the velocity must be zero. Consequently, the injected reactants velocity must decrease as they approach the closed end. This establishes a low velocity region in the vicinity of the closed end that apparently helps to stabilize the combustion process. The presence of the closed end forces the generated products and burning gas pockets to reverse their flow direction and exit the combustor through the large annular opening around the injector. The goal of this design is to evaporate and mix most of the liquid fuel with the air before burning, thus achieving pseudo premixed combustion at low temperature and, thus, low emissions. This approach has been pursued in this study because recent studies [7] with natural gas have shown that when burning in a non-premixed mode, the natural gas effectively premixes with the air before combustion takes place, thus reducing NO_x emissions when the global fuel-air ratio is lean.

As the stream of hot products flows out of the combustor (Fig. 1), it mixes with the incoming air in the shear layer that forms between the two flows. The mixing of the air with hot products increases its temperature, thus providing the energy needed for igniting the mixture. Additionally, the presence of radicals in the resulting mixture most likely reduces the mixture's ignition temperature, thus allowing combustion of leaner mixtures at lower temperature. The shielding of the fuel stream by the air prevents fuel from escaping into the out-flowing hot products before mixing with the surrounding air. This prevents the escaping fuel from burning at near stoichiometric, high temperature conditions that produce large amounts of NO_x and CO.

For practical applications, the SPRF combustor should operate with low CO and unburned hydrocarbons emissions, high combustion efficiency, low pressure losses, and no acoustic instabilities over a wide range of operating conditions. It would also be highly desirable if the combustor would offer these advantages when operated in a *non-premixed* mode, which is preferable to premixed mode of operation because it avoids some of the drawbacks of existing low NO_x, lean premixed combustors; e.g., flashback, lean blowout, and combustion instabilities. Particularly, it is desired to achieve this with liquid fuels, which is the focus of the present studies.

Figure 2 shows the experimental setup used in this study. The insulated combustor and injector location inside the combustor were identical to those used in the natural gas studies [6-9] to allow appropriate comparison of combustor performance burning liquid and gaseous fuels. The combustor consisted of a cylindrical quartz combustor insulated with alumina fiber. Thermocouples were used to measure the reactants temperature at the exit of the injector nozzle and the product temperature at the exit of the combustor. A Horiba PG-250 portable gas analyzer was used to measure the concentrations of NO_x, CO, O_2, and CO_2 in the exhaust flow. All NO_x and CO emissions were corrected to 15% excess oxygen. The air flow rate was measured using a thermal mass flow meter, the McMillan 50D-15C, and the fuel flow rate was determined from knowledge of the equivalence ratio obtained from measured concentrations of O_2 and CO_2 in the exhaust flow.

The rate of NO_x formation within the combustor is strongly coupled with temperature there, which is in turn affected by heat losses of the combustor. It is therefore important to determine whether the observed low NO_x emissions were due to combustor heat losses, which would provide unfairly low NO_x emissions. The conduction losses of the combustor were calculated using the maximum temperature difference of flame temperature and ambient conditions and, based on the low conductivity and large thickness of the insulation materials, were found to be negligible. Since the inner combustor wall was glowing red, though, it was important to determine losses due to radiation. The radiation heat losses from the combustor were estimated using a technique that utilized simultaneous gas sampling and temperature measurements [10] and is outlined in Appendix I: Heat Loss Estimate.

As noted earlier, the utilized injector and combustor designs (Fig. 2) place the liquid fuel stream inside the air stream. This serves to shield the fuel stream from the hot products when the reactants enter the combustor, thus preventing the onset of combustion until the reactants reach the low-velocity region near the closed end of the combustor. This design apparently produces nearly complete mixing of the fuel and air inside the combustor before combustion starts, thus preventing the need for any premixing devices and resulting in a lower weight combustor. The operation in nearly premixed condition near the flame zone implies that the maximum temperature in the reaction zone is not significantly higher than the adiabatic flame temperature of the global equivalence ratio, thus providing minimum prompt NO_x formation.

The studies presented in this paper used two fuel injector nozzles, noted as the straight-walled injector and "venturi injector" in Fig. 2. The straight-walled design consisted of two coaxial straight-walled tubes, the inner one carrying fuel and the outer one carrying air. Tests with this injector showed that with high enough air injection velocities, low NO_x and CO emissions could be obtained, due to the atomization quality of the blasting air. However, the high velocity comes at the cost of pressure loss across the injector. To counter this disadvantage, a "venturi injector" was developed that combined an airblast atomizer with a pressure recovery

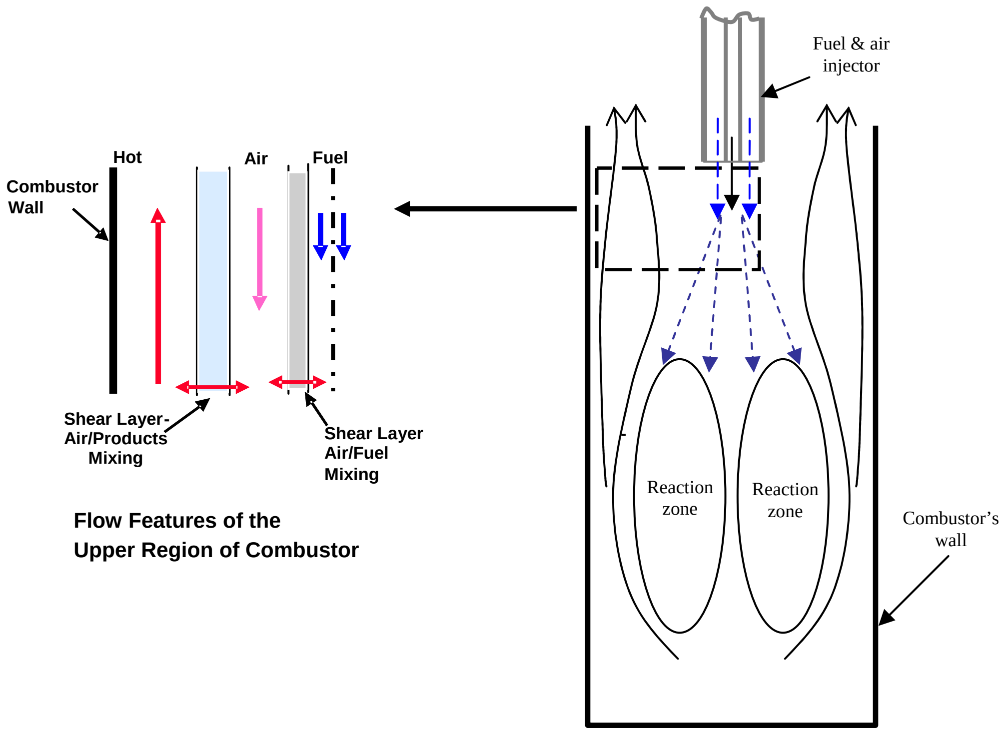

Figure 1. A schematic of SPRF (right) with the flow features of the upper region of the combustor (left).

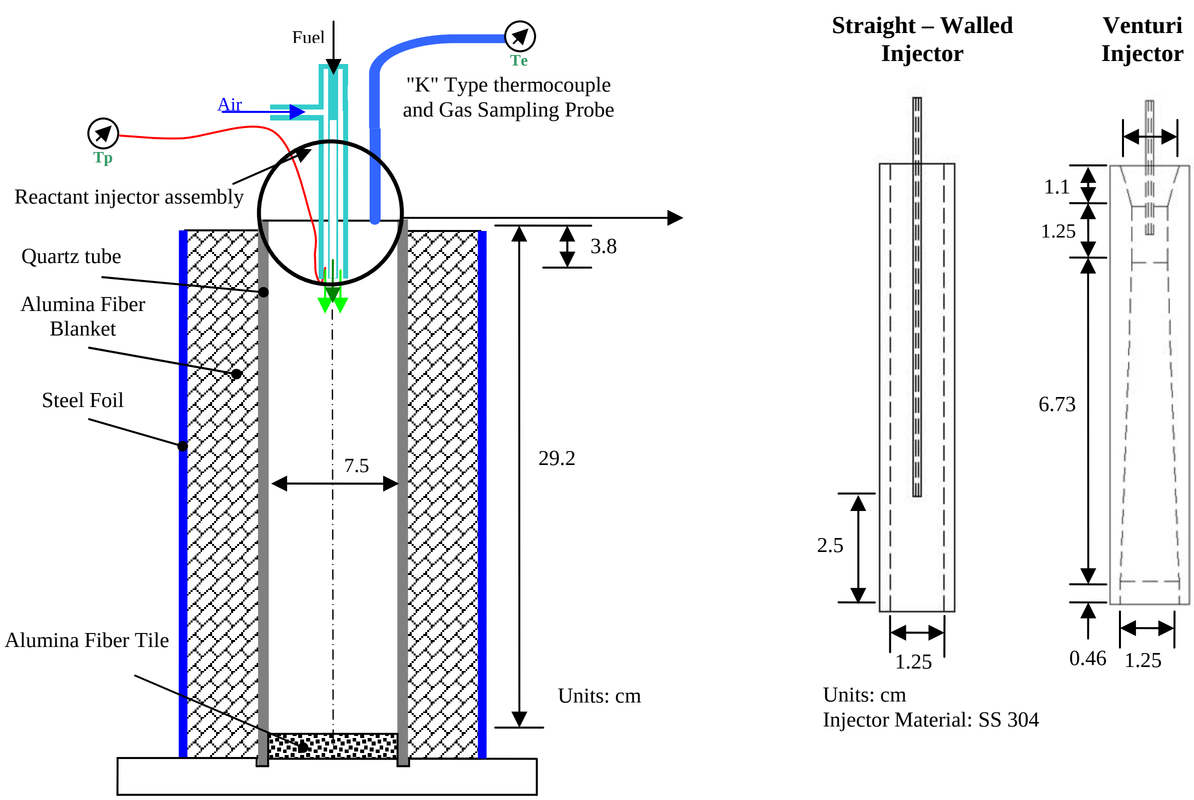

Figure 2. Experimental Setup for the SPRF combustor (left) and venturi injector (right).

diffuser. The throat area was set such that high subsonic flow was maintained over all flow rates tested (shown in Fig. 3) to eliminate pressure losses from shocks forming within the injector. Additionally, to allow for comparison with the straight-walled injector used in previous natural gas studies, the injector exit diameter was set to match the diameter of the straight-walled injector. With these design parameters set, the only parameters left to affect the injector effectiveness were the angles of the converging and diverging flow passages. Assuming turbulent flow, the converging and diverging angles were determined as a tradeoff between losses and injector length using basic turbulent pressure recovery charts [12]. Finally, note that the fuel line exit plane was placed at the nozzle throat (Fig. 2, right) where the air velocities and thus shearing forces were maxima.

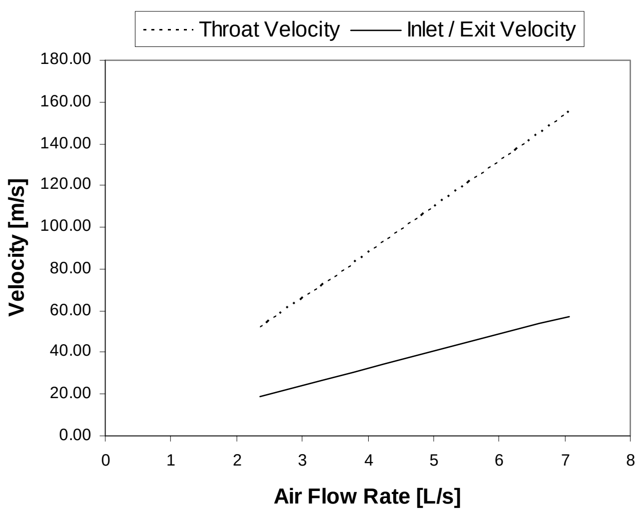

Figure 3. Calculated velocities in venturi injector at the throat and inlet and exit as a function of air flow rates under investigation.

RESULTS AND DISCUSSION

To investigate the trade-offs between pollutant emissions, pressure losses across the injector, and power density during the combustion of liquid fuels in the SPRF combustor, initial tests were performed at conditions that matched those used in the previous natural gas studies. The initial liquid fuel studies also used a straight-walled fuel injector in which liquid fuels (heptane and Jet-A) were supplied through a central injector tube (of smaller diameter) that previously supplied natural gas.

Emissions

Because thermal NO_x emissions depend exponentially upon the temperature inside the combustor, temperature provides the most objective criteria on which to base emission comparisons. Mentioned previously, for premixed natural gas combustion, the product temperature is only a function of preheat, stoichiometry, and combustor heat losses. As discussed before, the SPRF combustor heat losses were estimated to be less than 5 percent, so the NO_x emissions are only a function of preheat and stoichiometry. Since there was no external preheating of the reactants prior to combustion, further mention of preheating will pertain to the reactants being heating by the hot injector wall before entering the combustor or "internal preheating."

Straight-Walled Injector

Using the straight-walled injector, two cases were run using heptane fuel at two different air flow rates that corresponded to injection velocities of 43 and 130 m/s. The NO_x emissions dependence upon equivalence ratio for these two cases is shown in Fig. 5. Figure 5 indicates that increasing the air flow rate lowered NO_x over the equivalence ratio range. This trend can be explained by the effect that air velocity has on fuel atomization. At low flow rate and hence low air velocity the quality of the fuel atomization decreases, resulting in unmixedness, thus hot pockets, and ultimately an increase in NO_x production. Additionally, since incoming fuel droplets must stagnate and reverse, any large droplets that do not burn in the combustion region will instead hit the hot closed end wall and ignite instantly. This wall burning would likely generate locally elevated NO_x and CO. It is apparent that with lower air velocity more such "big droplets" are created, thus elevating the overall NO_x emissions. One could argue that decreasing flow rate would increase the reactants residence time in the combustor linearly, in turn increasing NO_x production. However, tests with premixed natural gas reported in [8] showed that the NO_x and CO emission characteristics with different flow rates were all but identical. This finding suggests that residence time may not significantly affect emissions.

In addition to the effect that the injector velocity has upon atomization, one should consider the effect that the air preheat has upon the initial vaporization of the fuel droplets. Figure 4 shows the discharge temperature of the straight-walled injector with heptane fuel. The discharge temperature was measured by a thermocouple hooked at the injector tip penetrating just upstream of the injector discharge (this thermocouple is shown in red in Fig. 2.) Figure 4 shows that with the higher velocity there was a consistent increase of 125°C in the discharge temperature. The higher temperature has two countering effects. On one hand, it increases the vaporization in the reactant stream seemingly providing for better premixing. On the other hand, higher preheat discharge temperature results in higher flame temperature and thus higher NO_x. One thus must conclude from the NO_x performance in Fig. 5 that the enhancement of atomization quality (augmented perhaps by better vaporization) far outweighs the effect of preheating.

In regards to the effect that the injector velocity has upon the discharge temperature, one may argue that increasing velocity decreases the residence time thereupon leaving less time for heat transfer and consequently lowering exit temperature. This contradicts the trend in Fig. 4. This apparent discrepancy is settled when taking into account that the increase in velocity also increases heat transfer between the reactants and the injector wall. Additionally, with an increase in the injector velocity comes an increase in the velocity of the exiting products thus also increasing the heat transfer from the hot products to the outside wall of the injector. The net result of the three effects is a moderate increase in the injector discharge temperature seen in Fig. 4.

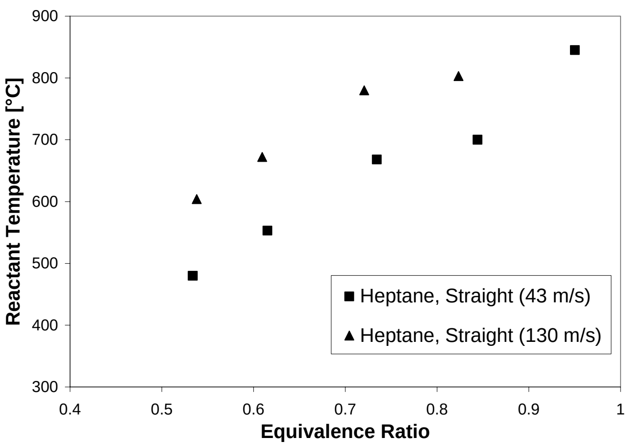

Figure 4. Temperature at the injector discharge as a function of equivalence ratio obtained with the straight-walled injector over various air flow rates burning heptane fuel.

Since the high flow rate showed lower NO_x for heptane investigations, the high velocity case was run again replacing the heptane fuel with the Jet-A fuel. This case was plotted in Fig. 5, which shows that the NO_x emissions were higher for Jet-A, although a minimum of less than 1 ppm was achieved near LBO. The higher NO_x may be attributed to atomization quality due to differences in the properties of the two fuels. Although higher emissions level are expected due to increase carbon to hydrogen ratio [13], it is alleged that most of the difference arise from degraded atomization due to higher viscosity of the Jet-A fuel, which is roughly twice that of heptane. The higher viscosity would decrease the effective atomization resulting in larger droplets and consequently higher NO_x. It is interesting to note from Fig. 5 that the emission characteristics of Jet-A with injection velocity of 120 m/s and heptane with 43 m/sec follow very closely. This agreement, though coincidental, suggests that the excess velocity counteracted the viscosity and provided nearly the same droplet sizes. Provided that the degraded NO_x emissions can be attributed mostly to atomization, it would be reasonable to assume that an increase in atomization quality would lower the NO_x generation. However, with injection velocity as high as 120 m/s the pressure losses are already significant and yield a non-practical system. This motivated the development of the venturi injector whose performance is described below.

Referring now to Fig. 6, the CO emissions collapse for all cases, attaining very low levels in wide range of operation. Although unburned hydrocarbons (UHC) were not measured in these studies, it is argued that the very low CO emissions indicate very low UHC as well. The lean blowout (LBO) is considered when the CO emissions increase sharply. Figure 6 indicates that the LBO was approximately the same for all air flow rates at 0.45. This low lean limit with no external preheating is attributed to the good flame stability of the SPRF combustor configuration.

As indicated above, low emissions could be achieved with straight wall injector through high air flow rates inducing high shearing velocity in the injector. Unfortunately, high discharge velocities lead to high pressure losses, which is unacceptable for practical combustors. The connection between the discharge velocity and the pressure losses can be derived through the isentropic flow relation,

$$u_0 = \left\{ \frac{2\gamma RT}{\gamma - 1} \left[1 - \left(\frac{p'}{P} \right)^{\frac{\gamma-1}{\gamma}} \right] \right\}^{0.5} \qquad (1)$$

where u_0 is the injector exit velocity, γ is the specific heat ratio, R is the gas constant, T is the total (or stagnation) temperature, p' is the total pressure of the combustor, and P is the total pressure of the air at the inlet of the injector [14]. Equation (1) is rearranged to yield

$$\left(\frac{\Delta p}{P} \right)_{\text{straight}} = 1 - \frac{p'}{P} = 1 - \left[1 - u_0^2 \frac{\gamma - 1}{2\gamma RT} \right]^{\frac{\gamma}{\gamma-1}} \qquad (2)$$

which provides a non-dimensional pressure loss across the injector. Figure 7 shows comparison of the predicted and measured pressure losses for the straight-walled injector in cold flow. To mitigate the high pressure losses of the straight-walled injector, a venturi-like injector was developed, described next.

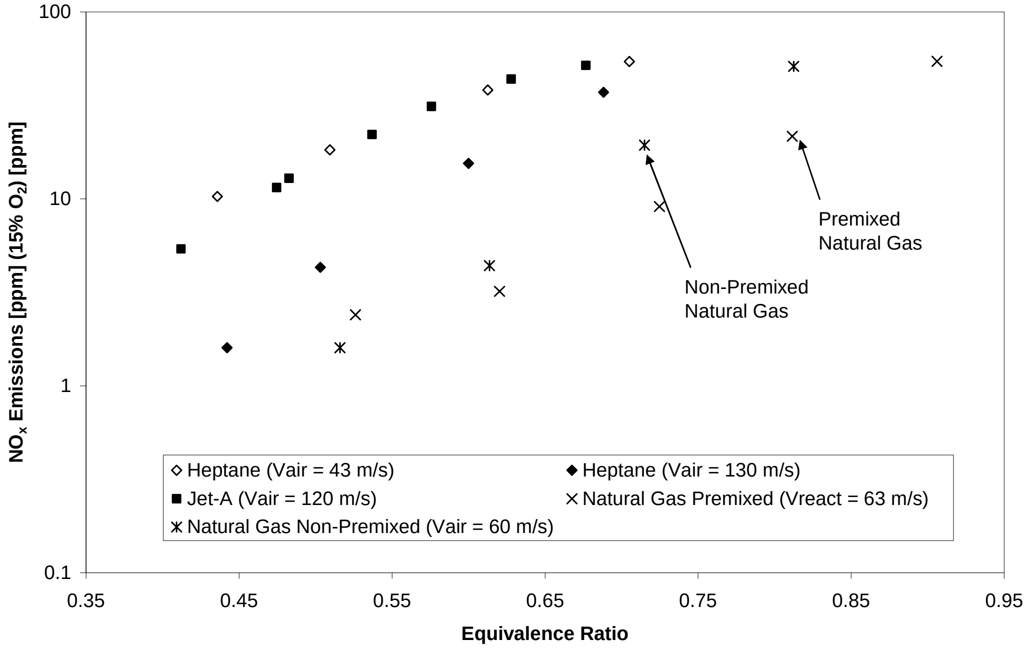

Figure 5. Corrected NO_x emissions (15% O_2) obtained with straight-walled fuel injector with Jet-A and heptane fuels for various discharge air velocities. Emissions with natural gas are shown for comparison.

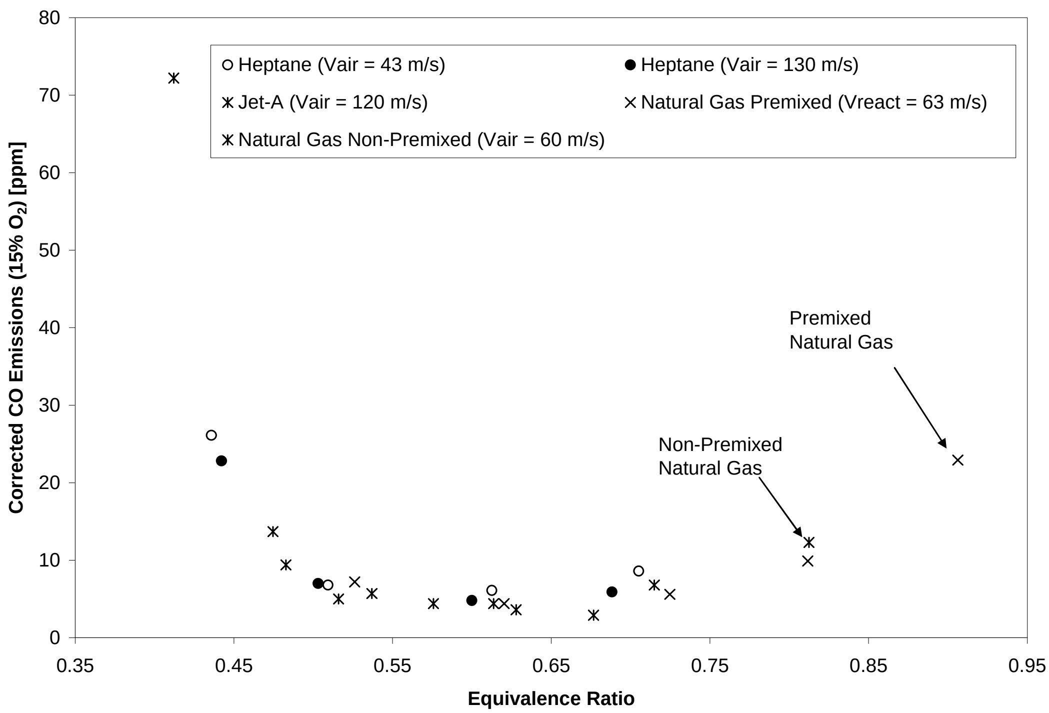

Figure 6. Corrected CO emissions (15% O_2) obtained with straight-walled fuel injector and Jet-A and heptane fuels for various air injection velocities. Emissions with natural gas operation are shown as well for reference.

Venturi Injector

The pressure losses over the venturi injector are obtained using Eq. 2 modified with the pressure recovery factor of the diffuser:

$$\left(\frac{P}{p'}\right)_{\text{venturi}} = \left(1 - C_P\right)\left[1 - u_0^2\,\frac{\gamma - 1}{2\gamma RT}\right]^{-\frac{\gamma-1}{\gamma}} \qquad (3)$$

where C_P is the pressure recovery coefficient. The theory for calculating the pressure recovery coefficient is given in [12] and, for the injector described in these studies, was 0.75. Figure 7 shows the predicted and measured pressure loss for the venturi injector.

Figure 8 compares the NO_x emissions obtained with venturi injector operating with Jet-A at various discharge velocities (ranging from 19-57 m/s) to that obtained with straight wall injector at injection velocity of 120 m/s. Emissions with premixed and non-premixed gaseous fuel are shown as well. Figure 8 shows that the emissions with the venturi injector are basically independent of the discharge velocity, and importantly, they are significantly lower than that obtained at high velocity with the straight-walled injector. We attribute this good performance to the fine atomization and, perhaps, the partial vaporization of the liquid droplets in the injector.

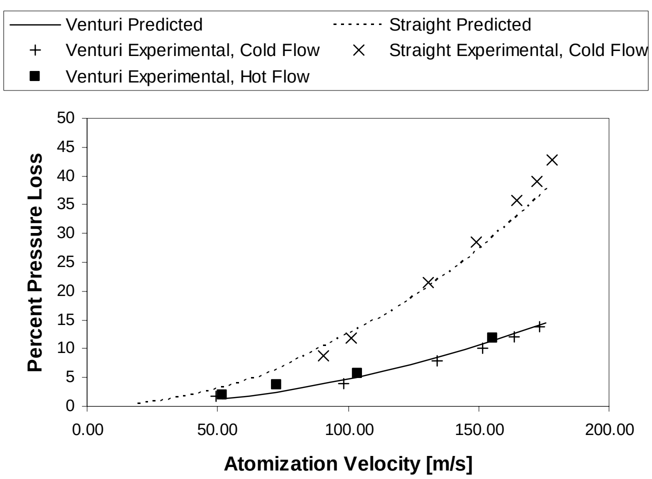

Figure 7. Predicted and measured pressure loss across the injector as a function of velocity at the atomization zone for the straight-walled and venturi injectors.

Figure 8 also shows that the Jet-A NO_x emissions are higher than that obtained with natural gas. While this is expected due to the higher carbon to hydrogen ratio [13], more research is required to determine what would be the minimum NO_x emission with Jet-A. It worth noticing that comparison of the emissions of non-premixed natural gas to the Jet-A venturi operation shows that the Jet-A emissions were not considerably higher. That could suggest that operation with pre-vaporized non-premixed Jet-A would not provide much lower emission than the venturi injector with liquid Jet-A.

Figure 9 shows the CO emissions for the cases shown in Fig. 8. In general the show the same behavior as the straight-walled injector. Interestingly, in spite of the prediction [13] that CO emission increases with increase in the carbon to hydrogen ratio, Fig. 9 actually indicates that the Jet-A operation produced slightly lower CO emissions than natural gas. Finally it is worth noting that both straight-walled and venturi injectors operating with Jet-A have the same LBO limit of 0.45.

A Note about Power Density

A so called sweet point of the combustor operation had NO_x emissions of 1-2 ppm, power density of 10 MW/m^3, and pressure losses of 5 percent operating non-preheated with an equivalence ratio of 0.55. Much higher flow rates and thus power density were readily obtained; in fact, the power density limitation in the current setup is the supply system rather than the combustor. As shown above, pressure losses vary nearly quadratically with the injector discharge velocity and thus with air flow rate. Thus, although much higher power densities could be attained, they come with excess pressure loss. Pressure loss of 5 percent is within the desired range for practical devices. It is interesting therefore to reflect the combustor at atmospheric conditions to elevated pressure operation in terms power density and pressure losses. Keeping the same temperature and velocity, density scales inversely with the operating pressure, thus, air mass flow rate will increase linearly with the pressure. It follow therefore that the attained power density with the same relative pressure losses scale linearly with the operating pressure. Consequently, at typical pressure ratio of 30:1 at sea level the reflected power density of the investigated combustor would be 300 MW/m^3. Much higher power densities of GW/m^3 and above (with low pressure losses) have already been achieved with the SPRF combustor under development and will be reported in following publications.

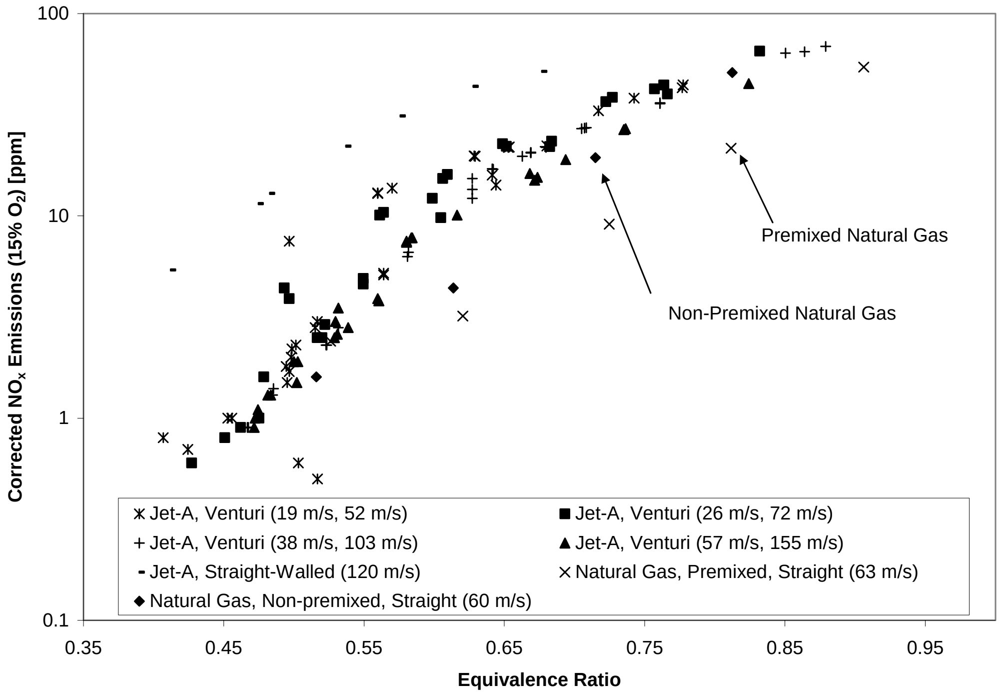

Figure 8. Corrected NO_x emissions (15% O_2) for the venturi injector with Jet-A fuel over various air flow rates. Both discharge and throat velocities in the venturi injector are indicated. Results obtained with the straight-walled injector operating with natural gas were included for comparison. In the non-premixed mode the velocity is that of the injected air whereas in the premixed mode the velocity is that of the reactants (both air and fuel).

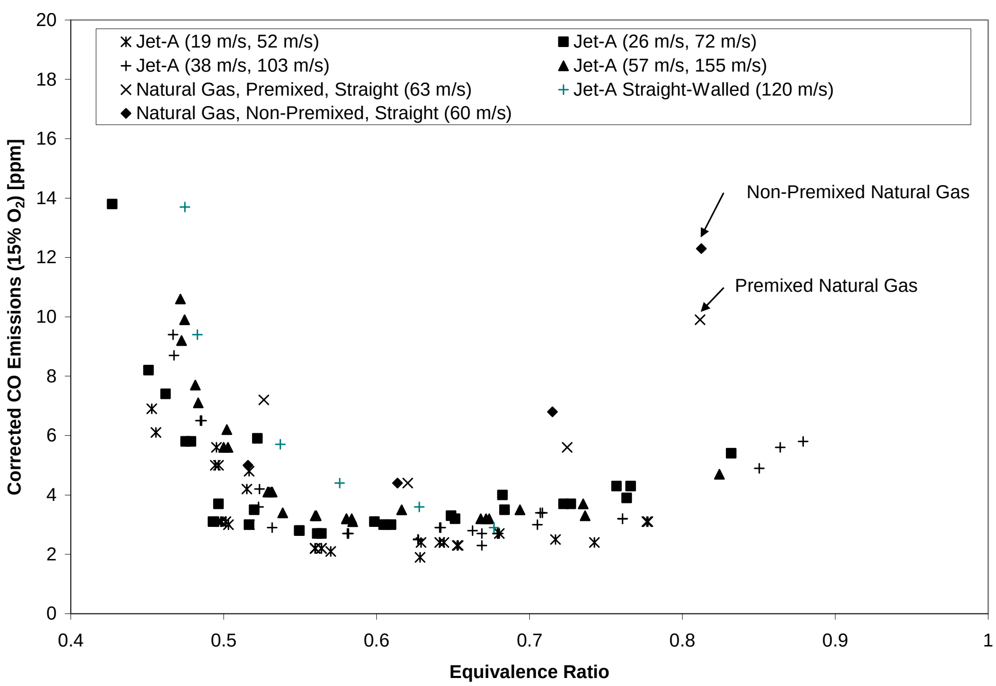

Figure 9. Corrected CO emissions (15% O_2) for the venturi injector with Jet-A fuel over various air flow rates. The velocity indications are as in Fig. 8.

CONCLUSIONS

This paper has explored the application of the SPRF combustor to liquid fuel combustion with low pressure losses. The combustor was shown to operate stably with ultra-low emissions, low pressure losses, and appreciable power density. The simplicity of the SPRF combustor and the ease at which it was adapted to liquid fuel operation suggests that it holds potential to the fields of propulsion, power generation, and heating.

It should be noted however that to materialize its potential for propulsion and power generation, the ultra-low emissions should be proven at high pressure. Also, the current configuration disregards issues of combustor wall temperature. Ongoing work with an all metal combustor cooled by the incoming reactant air is in progress. Also, further work is required for determining geometrical effects and scaling rules of the combustor.

Acknowledgements

This research was supported by NASA through the University Research, Engineering, and Technology Institute for Aeropropulsion and Power under Grant/Cooperative Agreement Number NCC3-982.

This research was also supported under the National Science Foundation Graduate Research Fellowship of John Crane.

REFERENCES

[1] Turrell, M. D., Stopford, P. J., Syed, K. J., and Buchanan, E., 2004, "CFD Simulation of Flow Within and Downstream of High-Swirl Lean Premixed Gas Turbine Combustor," GT2004-53112, Proc. of ASME Turbo Expo.

[2] Arai, M., 2000, "Flue Gas Recirculation for Low NO_x Combustion System," IJPGC 2000-15073, Proc. of ASME IJPC International Joint Power Generation Conference and Exhibition, Miami Beach, FL.

[3] Arai, M., 2000, "Flue Gas Recirculation for Low NO_x Combustion System," IJPGC 2000-15073, Proc. of ASME IJPC International Joint Power Generation Conference and Exhibition, Miami Beach, FL.

[4] Webster, T., John Zink Company, and TODD Combustion Group, Shelton, CT., 2001, "Burner Technology for Single Digit NO_x Emissions in Boiler Applications," Presented at CIBO NOx Control XIV Conference, San Diego, California.

[5] Kalb, J. R., and Sattelmayer, T., 2004, "Lean Blowout Limit and NOx-Production of a Premixed Sub-PPM NO_x Burner with Periodic Flue Gas Recirculation," GT 2004-53410, Proc. of ASME Turbo Expo.

[6] Neumeier, Y., Kenny, J., Weksler, Y., Seitzman, J., Jagoda, J., and Zinn, B. T., 2005, "Ultra Low Emissions Combustor with Non-Premixed Reactants Injection," AIAA 2005-3775, 41st AIAA/ASME/SAE/ASEE Joint Propulsion Conference, Tucson, AZ.

[7] Bobba, M. K., Gopalakrishnan, P., Radhakrishnan, A., Seitzman, J. M., Neumeier, Y., Zinn, B. T., Jagoda, J., "Flame Stabilization and Mixing Studies in a Novel Ultra-Low Emissions Combustor," AIAA-2006-0963, 44th AIAA Aerospace Sciences Meeting and Exhibit, Reno, NV, Jan 9 – 12, 2006.

[8] Crane, J. M., Neumeier, Y., Jagoda, J., Seitzman, J. M., Zinn, B. T., "Effect of Internal Heat Transfer and Combustor Dimension on Performance of the SPRF Combustor," work in progress to be published at 42nd AIAA/ASME/SAE/ASEE Joint Propulsion Conference, 2006.

[9] Gopalakrishnan, P., Undapalli, S., Bobba, M., Sankaran, V., Menon, S., Zinn, B. T., Seitzman, J., "Measurements and Modeling of the Flow Field in an Ultra-Low Emissions Combustion," AIAA-2006-0962, 44th AIAA Aerospace Sciences Meeting and Exhibit, Reno, NV, Jan 9 – 12, 2006.

[10] Neumeier, Y., 2005, "Correcting Thermocouple Reading Using Oxygen Content Reading," Georgia Institute of Technology, Internal Technical Document.

[11] Turns, S., "An Introduction to Combustion," McGraw-Hill, 2000.

[12] Fox, R., and McDonald, A., 1998, Introduction to Fluid Mechanics, John Wiley and Sons, New York, NY pp. 364-365.

[13] Malte, P. C, Edmonda, R. G., Lee, A. C., Novosselov, I., and Bruyn Kops, S., "The Staged Prevaporizing-Premixing Injector: High Pressure Evaluation", Advanced Gas Turbines Systems Research Final Report, Clemson, SC, December 2002, p. 26 – 27.

[14] Rutar, T. (as Shuman, T. Rutar) 2000, "NO_x and CO Formation for Lean-Premixed Methane-Air Combustion in a Jet-Stirred Reactor Operated at Elevated Pressure," PhD Thesis, University of Washington, Seattle, Washington, p.31.

APPENDIX I: HEAT LOSSES ESTIMATE

The combustor heat losses can be readily determined if accurate temperature measurement can be achieved at the exit plane of the combustor where hot products are discharging. Such an accurate temperature measurement is not easily obtained with a thermocouple because of significant radiation and other losses from the thermocouple. In this study, an accurate temperature was determined using a combination of a thermocouple and gas analyzer. Specifically a co-located thermocouple and gas analyzer probe were traversed upwards along a path were hot products were mixing with ambient air. As the distance from the combustor discharge increased, the dilution of the exhaust flow by ambient air entrainment increased, thus decreasing the mixture temperature and increasing the O_2 concentration, as shown in Fig. 10. At a sufficiently long distance from the combustor, the exhaust gases were cooled to a level where thermocouple losses were negligible, thus providing the correct gas temperature there. Using enthalpy balance, the correct temperature could be retraced backward based upon the far field measurement. Figure 10 shows the reconstruction of temperatures for two combustors. The first combustor was double walled with the incoming air streamed between casing and outer wall prior to entering the combustion chamber. The very low temperature of the external wall prevented convection and radiation losses and the relatively low temperature of the casing minimized radiation losses. Consequently this combustor experienced low heat losses. Figure 10 shows that the zero losses temperature regression line and the far field measured temperature coincide, confirming the negligible losses. The temperature difference between the regression line and the measured points illustrates, then, the heat losses of the thermocouple for this case. The other combustor also used a double wall, but in its case, water was streamed between the walls thus removing a significant amount of heat. Figure 10 shows that the regression line that matches the far field temperature corresponds to 30 percent losses. Using this technique the investigated combustor heat losses were estimated to be at most 5 percent. A more detailed discussion of this approach will be published at a later date.

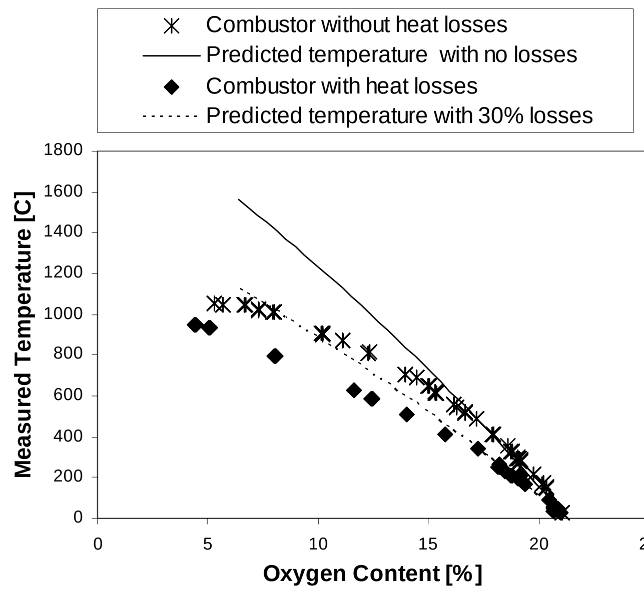

Figure 10: Measured temperature for varying distance from the combustor exit plane as a function of oxygen content